Int. J. Electrochem. Sci., 8 **(2013)** 6553 - 6565

International Journal of
ELECTROCHEMICAL
SCIENCE
www.electrochemsci.org

Influence of Fluoride and Chromium(VI) ions on Corrosion Mechanisms of Pb-3wt%Sn-0.5wt%Ag Anode

Jianzhong Li[1,*], *Xiuli Sun*[1], *Yanwen Tian*[1], *Yue Zhao*[2]

[1] School of metallurgy and materials, Northeastern University, Shenyang 110004, China
[2] MMM School, Faculty of engineering, University of Wollongong, NSW 2522, Australia
[*]E-mail: lijz@smm.neu.edu.cn

Received: 29 March 2013 / *Accepted:* 15 April 2013 / *Published:* 1 May 2013

A mix solution of fluorine and chromium ions (Cr-F solution) for applications in chromium plating field has a characteristic of strong corrosion and oxidation, promoting lead alloys anode degraded rapidly. The present study explores the time dependence on corrosion mechanisms of lead alloys anode oxidised in Cr-F solution under conditions of high current density. Scanning electron microscopy (SEM) with an energy dispersive X-ray spectroscopy (EDX) shows a double-layer oxide film is electrochemically developed on lead alloys anode after oxidation for above 0.5h. The outer layer is primarily PbO and PbO_2, and the inner layer contains $PbCrO_4$ and PbF_2, followed by PbO. In the initial oxidation stage (oxidation time below 60s) of lead alloys anode, the Raman peaks of $PbCrO_4$ and PbF_2 are clearly shown by the Raman spectra scanning. With increasing reaction time, Raman peaks intensity for PbO is strengthened. Cyclic voltammetry reveals that effect of fluorine ions on the electrode potential for lead alloys anode change among Pb, PbO, $PbCrO_4$, PbO_{1+x} ($0<x<1$) and β-PbO_2. After oxidation treatment, electrochemical impedance spectroscopy (EIS) in 3g/L NH_4F and/or 170g/L CrO_3 solution indicates greater charge transfer resistance (R_t) for samples of longer oxidation time up until 2h. The corrosion mechanisms of the anode reaction at the anode/solution interface are discussed using the experimental results.

Keywords: lead alloy, anode, corrosion mechanism, high current density, chromium plating

1. INTRODUCTION

The use of lead base alloys as anode material are widely considered in industrial hydrometallurgical process, such as chromium plating [1], electrowinning [2-3] and lead-acid batteries [4-5], due to low corrosion rates, high electrocatalytic efficiency and electrical conductivity[6-7]. In addition, most hydrometallurgical process uses sulphuric acid solution. These attractive properties have been a driving force for the early research of lead base alloys and their corrosion mechanism in sulphuric acid solution [8-10].

For conventional chromium plating field, the electrolyte consist of not only sulphuric acid, but also the high concentration of chromic acid with 250 g/L CrO_3 [11]. Hence, some researches indicate corrosion rate and layers structure on the electrode of lead base alloys in chromium-included solution. Hine et al. [11] reported the corrosion rate of the lead alloys in the electrolyte is in the range 1-10 mg/Ah, depending on the alloy compositions. McBurney et al. [12] proposed that in chromic acid a passive film of $PbCrO_4$ forms at very low overpotential and the formation of PbO_2 is fixed at about 1.5V overpotential. However, conventional chromium plating technology shows the current efficiency for chromium deposition is low, about 10% or less. Metal deposition no longer takes place if the electric circuit is once interrupted. Therefore, the conventional chromium plating is inadequate for some applications.

Of the modified solution containing fluorine compound, the ammonium fluoride bath, consisting of low concentration of CrO_3 and NH_4F, is most popular, although other electrolytic solution, such as those containing fluoborate or fluosilicate, for example, are also used. The main reason is that current efficiency for metal deposition from the ammonium fluoride bath increases to above 20% compared to that from conventional chromium plating because of the difference of the catalytic activity in both solutions. However, the problem is presented that the anode consumption in fluoride-included solution is great. According to Hine et al. [11] reports, the corrosion rate of a Pb-2%Sn alloy anode in the conventional plating bath and the fluoride-included bath are 5 and 12 mg/Ah, respectively, under normal conditions. With the plant experiences, the grain boundaries of alloy are attacked, fine particles go away into the solution, and a part of these solids precipitate on the cell bottom which is troublesome for the cell operation. This causes a significant increase of energy use during metal production. Other problems encountered with lead alloys are high costs of some alloying elements, corrosion and subsequent contamination of cathodes [13-14]. Numerous previous investigations[8-10, 15-16] aiming for the improvement of Pb anodes' corrosion resistance focus on the inclusion of various alloying additives in the lead anode to achieve better mechanical properties and/or finer-grained and more homogeneous microstructure. However, few reports regarding corrosion mechanism of lead alloys anode in Cr ions and F ions solution at high current densities of above $10A/dm^2$ are available in literature.

The main objective of the present study is to explore the effect of oxidation time of lead alloys anode in Cr and F ions solution on oxide film properties, as well as the surface reaction mechanism in the initial oxidation stage of lead alloys anode under conditions of high current density. To investigate how the behaviour of oxide film on lead alloys surface are affected by Cr ions or F ions, the corrosion behaviour of lead alloys anode was studied in Cr ions or F ions solution by electrochemical impedance spectroscopy (EIS) and cyclic voltammetry (CV).

2. EXPERIMENTAL

The substrate material used in the research was a Pb-3wt%Sn-0.5wt%Ag ingot-cast alloy for commercial anode applications of tin free steel, which can be used as the substitution of tinplating in various industrial applications, involving in the packing materials for good and drink products,

automotive parts and construction materials [17]. Rectangular substrates with dimensions of 50 mm×40 mm×8 mm were used in the research. The substrates were mechanically polished with emery papers up to 1000 grit to ensure similar surface roughness. The polished substrates were thoroughly washed with acetone and distilled water before passing through the plating procedure as the anode.

After polishing, the lead alloys anode were treated in 170g/L CrO_3 and 3g/L NH_4F solution (*i.e.*, the standard concentration range of tin free steel production; a low carbon steel was used as cathode to set up electrolysis system) under current density of 20A/dm^2 at different time of 0.5, 1, 1.5, 2 and 2.5h, respectively. Subsequently the samples were sonciated in deionzied (DI) water and in ethyl alcohol prior to XRD analysis. XRD (Rigaku D/ max-rA X-ray diffractometer) was used to investigate crystallinity of the oxidation coatings. X-ray profiles were measured between 10 and 80 deg. (2μ angle) at 45 kV and 40 mA with Cu K-alpha radiation source. The scanning speed and space length were 8 deg./min and 0.02 deg., respectively. The samples were removed from the XRD after scanning so that they could be analysed next to observe their cross-sections morphology under the same conditions via a scanning electron microscope (SEM). X-ray spectroscopy analysis was used for determining the distribution content of the oxidation coatings cross-sections.

To study the surface reaction mechanism in the initial oxidation stage of lead alloys anode, Raman spectrum measurements were performed on a Jobin Yvon HR800 Raman Spectrometer system equipped with a 633 nm He-Ne laser. The power of the exciting laser measured at the sample position was about 10–25 mW. Firstly, Raman spectrum was used to investigate the Raman properties of 170g/L CrO_3 solution (Cr solution) or the mix solution of 170g/L CrO_3 and 3g/L NH_4F (Cr-F solution), respectively. And then, the polished lead alloys anode without oxide films were chemically treated by steeping in these solution for 3s. After the steeping, the samples were rinsed with DI water and air-dried. Raman spectrum scanning examined the samples to observe the Cr and F ions adsorption on anode surface. Removed from the Raman Spectrometer after scanning, the samples could be treated electrochemically again in these solution allowing the treating progress of the same position to be observed for 10, 20 and 60s of oxidation treatment under density current of 20A/dm^2. Samples were also examined by Raman spectrum after continuous oxidation treatment but no difference were observed between the resulting surface properties from the two methods. The Raman spectra of the samples were recorded at room temperature via long-focus lens for 50 times.

Cyclic voltammetry, AC impedance measurements were performed in a conventional 250mL three-compartment Pyrex cell using electrochemical workstation, model PARSTAT 2273(American Princeton Company). A defined sample area of 2 cm^2 was exposed to the electrolyte, and all the current value was normalized to the geometrical surface area. A luggin capillary was placed near the working electrode to minimize the solution resistance. A platinum foil was used as counter electrode, and a saturated calomel electrode (SCE) was used as reference electrode. All electrode potentials were referred to SCE if no otherwise stated. Cyclic voltammetry tests were carried out at room temperature (25±1 ^{0}C) under conditions of potential range from -1.5V to 2V with the frequency of 1000Hz and sweep rate of 2mV.s^{-1}. Electrochemical impedance spectroscopy measurements were performed in a frequency range of 10^5 Hz to 10^{-1} Hz with ten points per decade and a sine wave with 10mV amplitude was used to perturb the system. The impedance data were analyzed and fitted with the simulation Zsimpwin equivalent circuit software.

3. RESULTS AND DISCUSSION

3.1 Corrosion process of lead alloys anode surface under electric field

In order to study corrosion reaction from Cr and F ions to lead alloys under conditions of electric field, the properties of oxide film on lead alloys anode surface are studied in Cr-F solution at different oxidation time. Fig.1 shows cross section SEM and EDS elements line scan of oxide film on lead alloys anode surface under current density of 20A/dm^2 at different oxidation time of 0.5, 1, 1.5, 2 and 2.5h, respectively. Oxide film at 0.5h with a thickness about 6μm is continuous and uniform. It is conspicuous in Fig. 1(a) that the oxide is Pb/O-rich close to the surface of oxide film and Cr/F rich near oxide-lead substrate interface. It is apparent, from the cross section SEM, that up until 2h of oxidation time, the thickness of oxide film increase continuously to about 16μm. In addition, oxide grains grow roughly and the oxide film becomes gradually looser, existing minor porosity. However, during further oxidation of 2.5h, these structures are separated from the oxide film with decreasing a thickness to about 5μm, and since some of cracks are generated in oxide film and they are only loosely interconnected with each other, they become disconnected from the sample surface and fall into the solution. As can be seen in cross section EDS elements line of further oxidation, a double-layer oxide structure with a Cr/F-rich inner layer and a Pb/O-rich outer layer is observed on lead alloys anode surface. In comparison, the oxide film on lead alloys surface at 2.5h exhibits a distribution and a thickness similar to that at 0.5h. It can be concluded that the oxide film is broken off and Cr/F rich near oxide-lead substrate interface reappears easily. Fig. 2 gives XRD patterns of oxide film on lead alloys anode corresponding to the conditions of above SEM. The diffractograms of oxide film at 0.5 and 1h show the presence of PbO and lower intensity of the diffraction lines for PbO_2, PbF_2 and $PbCrO_4$ peaks. The peak intensity of PbO_2 is higher for oxide film at 1h than for oxide film at 0.5h. The peaks intensity of $PbCrO_4$ and PbF_2 are lower for oxide film at 1h than for sample at 0.5h oxide film. This means that oxide film at 1h contains less quantity of $PbCrO_4$ and PbF_2. XRD patterns of oxide film at 1.5 and 2 h show a better crystalline part of PbO_2 and PbO, and the diffraction peaks of $PbCrO_4$ and PbF_2 almost disappear.

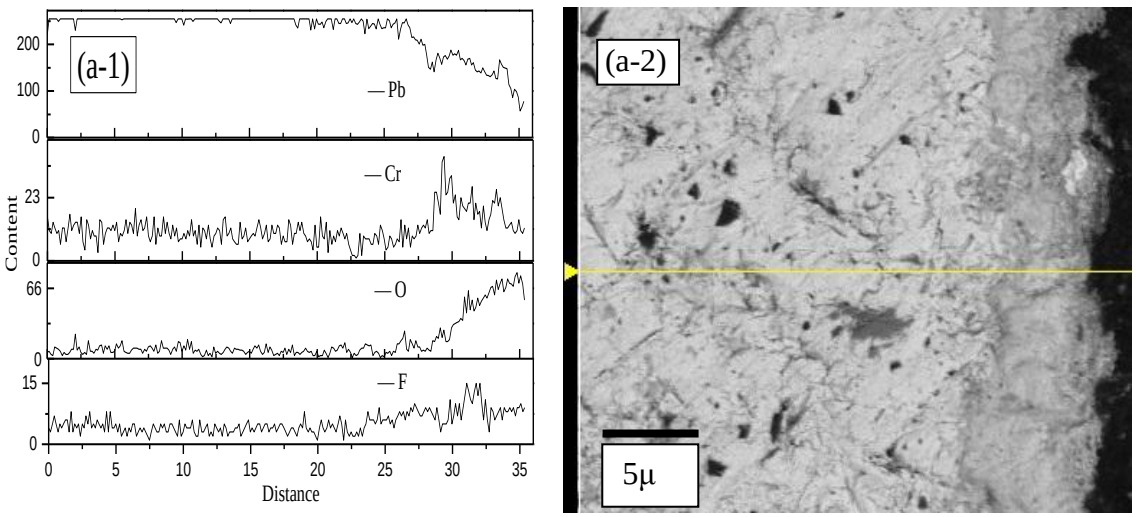

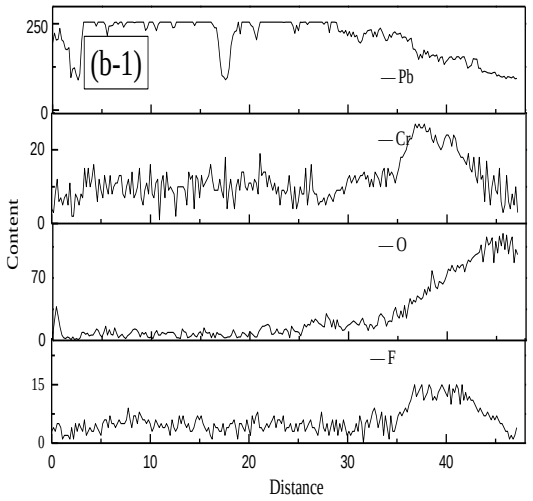
(b-1)
Pb
Cr
O
F
Content
Distance

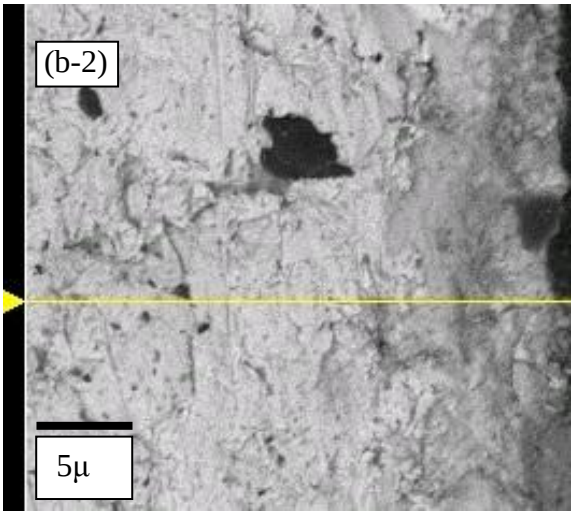
(b-2)
5μ

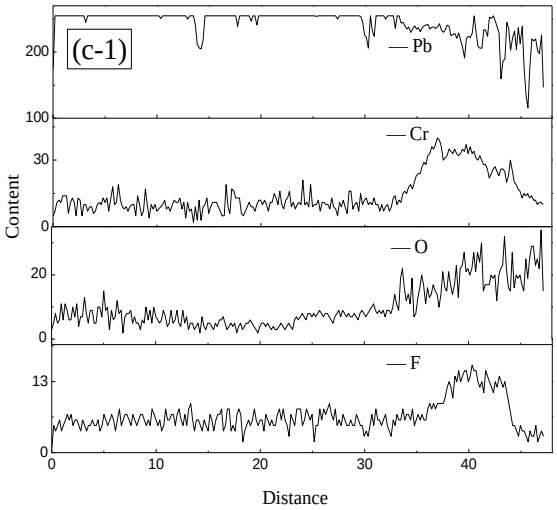
(c-1)
Pb
Cr
O
F
Content
Distance

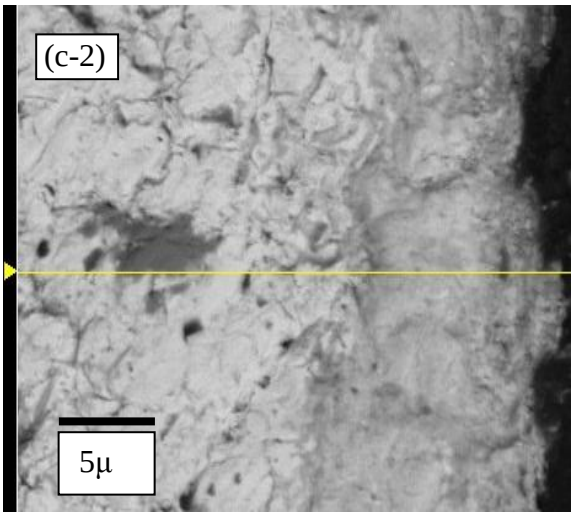
(c-2)
5μ

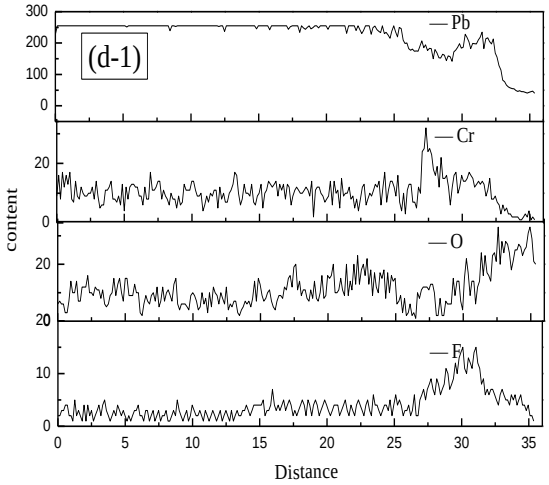
(d-1)
Pb
Cr
O
F
content
Distance

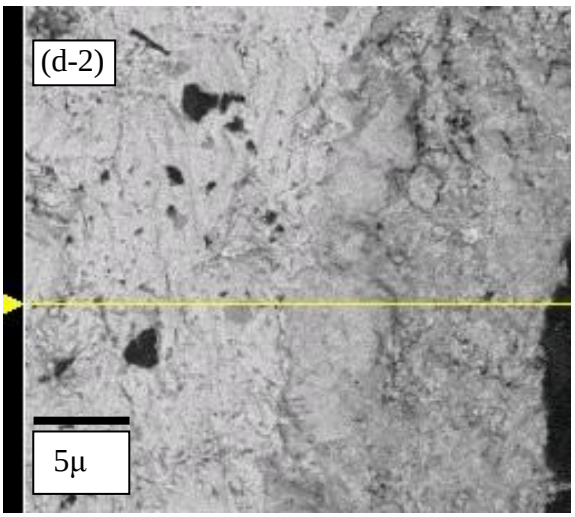
(d-2)
5μ

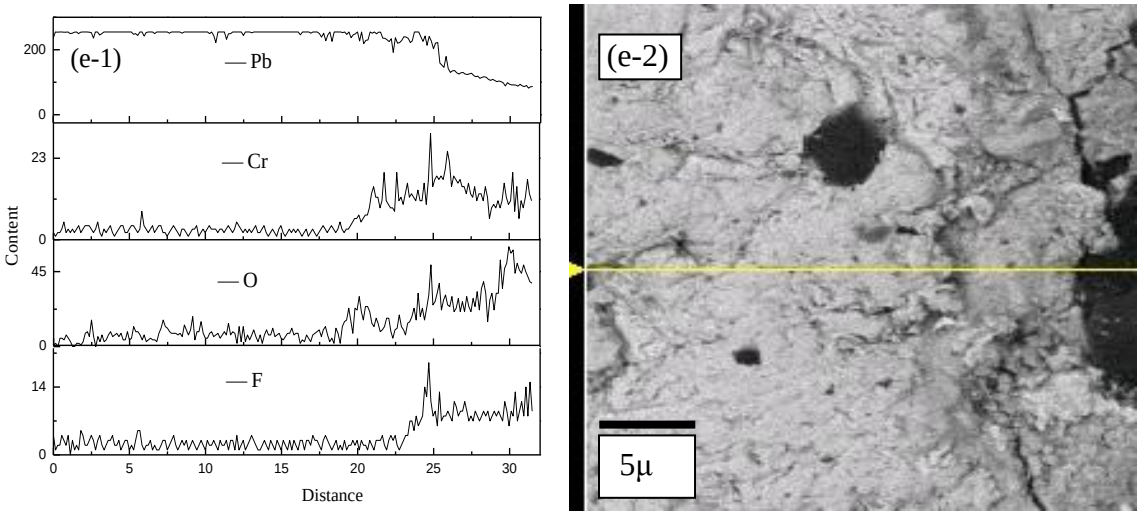

Figure 1. Cross-sections morphology and EDX of lead alloy surface treated by electrolysis in 170g/L CrO_3 and 3g/L NH_4F solution under different oxidation time of 0.5, 1, 1.5 2 and 2.5h

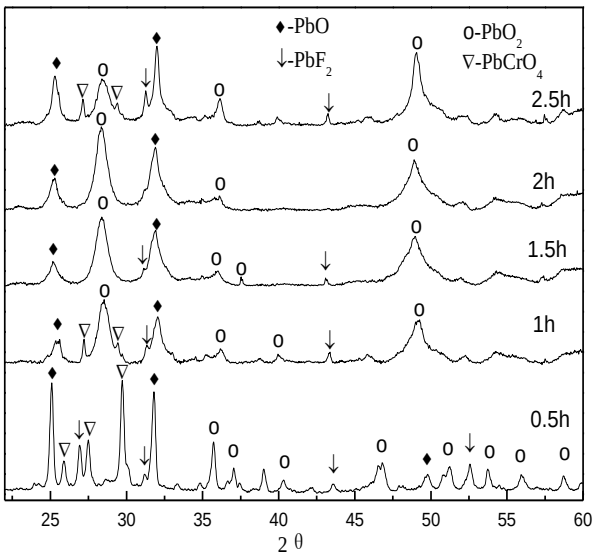

Figure 2. X-ray spectra of lead alloy surface treated by electrolysis in 170g/L CrO_3 and 3g/L NH_4F solution under different oxidation time of 0.5, 1, 1.5 2 and 2.5h

But when oxidation time increases to 2.5h, diffraction peaks of $PbCrO_4$ and PbF_2 are presented again, though a crystalline of PbO_2 and PbO remains better. It can be admitted that the crystalline features of the different oxidation time are much more evident for the different corrosion products on oxide film at 1, 1.5 and 2h than on oxide film at 0.5 and 2.5h, indicating generally the presence of more important corrosion products of $PbCrO_4$ and PbF_2 oxide film at 0.5 and 2.5h.

3.2 Cr and F ions action in the initial corrosion of lead alloys anode under electric field

In order to understand the influence of chromium and fluorine ions on the surface reaction mechanism in the initial oxidation stage of lead alloys anode under conditions of high current density,

Raman spectrums for the different solution and the lead alloys anode treated after different conditions were recorded and shown in Fig.3. As can be seen in Fig.3 (a), the Raman spectrums for Cr solution and the Cr-F solution are both dominated by two Raman bands at ~848 and ~910 cm^{-1}. These spectrums were previously assigned to terminal Cr=O vibrations of monochromate (1000 cm^{-1}) and bridging Cr-O-Cr vibrations of polychromate (845cm^{-1}) species reported by M. M. Hoffmann et al. [18]. Detection of surface chromium oxide bands of ~ 910 cm^{-1} is below bands of 1000 cm^{-1} terminal Cr=O vibrations of monochromate due to hydrogen bond absorbed by Cr=O to form Cr=O–H. In addition, it is evident that fluorine ions have no significant effect on the Raman spectrums for Cr solution. In Fig.3 (b), after lead alloys anode steeping in Cr solution or Cr-F solution for 3s without electric field, respectively, a similar set of experiments to obtain the Raman spectrum was carried out on lead alloys anode surface. Compared with Fig.3 (a) and (b), it can be seen that the dehydrated Raman frequencies are nearly same with that of Cr solution and Cr-F solution. But Raman spectrum intensity ratio of ~848 cm^{-1} to ~910 cm^{-1} for lead alloys anode is higher than that of Cr solution and Cr-F solution. Furthermore, Raman spectrum intensity ratio of ~848 cm^{-1} to ~910 cm^{-1} for lead alloys anode treated by Cr-F solution is higher than that treated by Cr solution. As mentioned in previously my work [19], according to bands of ~848 cm^{-1} is corresponding to $Cr_2O_7^{2-}$ and bands of ~910 cm^{-1} is of $HCrO_4^-$, chromium ions absorbed on lead alloys anode surface happen, and $Cr_2O_7^{2-}$ absorption is stronger than $HCrO_4^-$ under the low CrO_3 concentration. The Fig. 3(b) results indicate that F ions promote adsorption free energy of $Cr_2O_7^{2-}$ and increase the Raman spectrum intensity of ~848 cm^{-1}.

However, when lead alloys anode is working under electric field at different time, using Cr-F solution and Cr solution as electrolyte, respectively, the dehydrated Raman spectrums make a big different in Figs.3(c), (d). As to Cr-F solution as electrolyte, up until oxidation time of 60s, Raman spectrum intensity of ~900cm^{-1} is always lower than that of ~837cm^{-1} on lead alloys anode surface, though Raman spectrum intensity of ~900cm^{-1} increases with oxidation time . When electrolyte is changed to Cr solution, Raman spectrum intensity of ~900cm^{-1} is appreciably higher than that of ~837cm^{-1} for lead alloys anode surface under oxidation time of 10s. As increasing oxidation time to 60s, Raman spectrum intensity of ~900 cm^{-1} is continually increased.

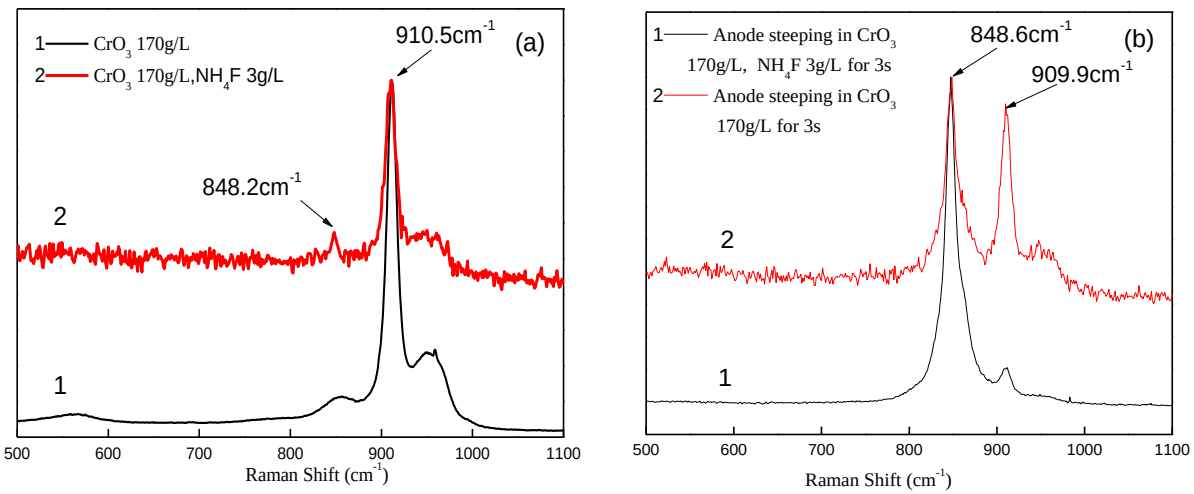

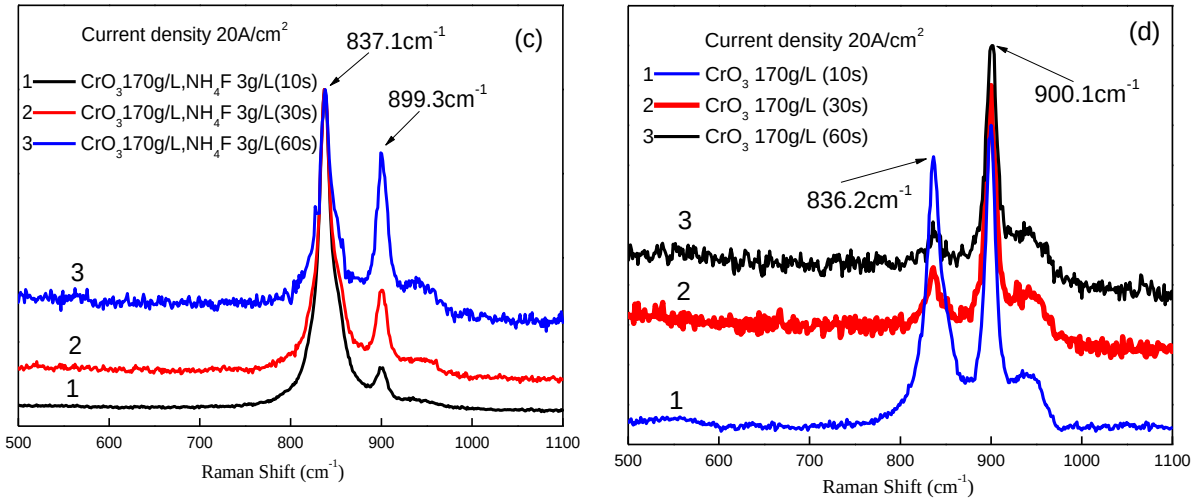

Figure 3. Raman spectrum for (a) the different electrolyte solution, (b) the etched lead alloy surface, (c) the lead alloy after oxidization in Cr-F solution at different time of 10, 30 and 60s and (d) the lead alloy after oxidization in Cr solution at different time of 10, 30 and 60s

Combined with SEM, XRD and elements line scan analyses above, the presence of a new Raman band at ~837 cm^{-1} is corresponding to $PbCrO_4$ and PbF_2 formation in Cr-F solution, but is $PbCrO_4$ in Cr solution (the reasons reported in reference [19]).

Similar observations for $PbCrO_4$ Raman band at ~840 cm^{-1} and PbF_2 Raman band at ~869 cm^{-1} have been reported in the literature of P. Thangadurai' [20] and E. Bandiello'[21], although the blueshift in Raman frequencies are observed due to lattice expansion. Another new Raman at ~900 cm^{-1} is corresponding to a PbO formation, which evidence is obtained that a better crystalline part of PbO is growing with oxidation time in the initial oxidation XRD in Fig.2. These suggest that when electrolyte is Cr-F solution, the main compositions of the initial corrosion film contain $PbCrO_4$ and PbF_2 on lead alloys anode surface under electric field. With increase of oxidation time, PbO with a better crystalline dominates quickly the main compositions of the corrosion film and develop gradually PbO_2, although PbO is reacted slowly with fluorine ions to form PbF_2.

3.3 Corrosion mechanism of Cr ions cooperated with F ions to lead alloys anode under electric field

Fig.4 shows the cyclic voltammograms of lead alloys anode in different ions solution under different conditions. Lead alloys anode are researched in two forms: the new lead alloys anode (in Fig.4 (a), (b) and (c)) and the lead alloys anode with oxide film under oxidation time of 0.5, 1, 1.5, 2 and 2.5h, respectively (in Fig.4 (d)). It is showed from Fig.4 (a) that anodic peak is presented at peak potential of -0.2V, no cathodic peak there. According to the literatures [8-9], the peak is assigned to the oxidation of Pb to PbO. While lead oxide, as an instable oxide, might be easily eroded by F^- ions in reductive process, leading to no reduction of PbO to Pb. For CV curves of the new lead alloys anode in Cr ion solution in Fig.4 (b), the asymmetry between the oxidation and reduction process can be seen. Anodic peaks b_1, b_2, b_3 are observed at peak potential of -0.2V, 0.2V and 1.3V, respectively. Peak b_1 is believed to be corresponding to the oxidation of Pb to PbO, and b_2 the chemical reaction of Pb, PbO or

$PbCrO_4$ to PbO_{1+x} ($0<x<1$) [22]. While peak b_3 is very likely to be corresponding to the reaction to form β-PbO_2 from $PbCrO_4$, PbO_{1+x} or a little Pb. For cathodic scanning of Cr ion solution, cathodic peaks b_4 and b_5 are obviously found at peak potential of 1.35V and -0.6V, respectively, which should be corresponding to β-PbO_2 be reduced to $PbCrO_4$ and $PbCrO_4$ to Pb, respectively. When F ions are added into Cr ions solution, cathodic peak b_4 disappears in CV curves of the new lead anode (see Fig. 4(c)). The results indicate that the low valence lead oxide film is formed easily on the new lead anode surface in Cr-F solution. With increasing oxidation potential, lead suboxide oxidise slowly to high valence lead oxide, forming oxide film with a thin thickness under low current density. And the thin oxide film at the interface is not stable enough to provide better corrosion resistance. In addition, the oxidation time was very short so the oxide film did not completely cover the whole surface. As a result, a thinner oxide film formed on lead alloys anode surface is eroded easily to crack or break by fluorine ions in the reduction process, exposing the underneath fresh lead surface to the electrolyte, due to strong corrosion characteristics of fluorine ions. This causes no reaction process of β-PbO_2 reduction to $PbCrO_4$.

However, lead alloys anode with oxide film under different oxidation time, show completely different CV curves, as indicated in Fig.4 (d). Compared with Fig.4(b), (c) and (d), cathodic peaks for lead alloys anode with oxide films at 0.5, 1, 1.5, 2, and 2.5h, respectively, are presented at the similar peaks potential. In addition, anodic peaks for samples with oxide films at 0.5 and 1h increase peaks potential to positive direction, and disappear for samples with oxide film at 1.5 and 2h. For CV curves of lead alloys anode with oxide film at 2.5h, cathodic and anodic peaks are observed again at potential of -0.8V, -0.2V, and 1.3V, respectively. Lead alloys anode after oxidation at above 0.5h is completely covered by oxide film containi ng lead oxide, lead chromate and minor lead fluoride, and the thickness for samples oxide films are at least 5μm, as indicated in Fig.1. Because fluoride ions can not destroy the thick oxide film in a relatively short time, the process of β-PbO_2 reduction to $PbCrO_4$ or PbO_{1+x} is presented in cyclic voltammetry. For anodic peaks for samples at 1.5 and 2h disappearing, the reasons is that the oxide films consist primarily of lead dioxide with a better crystalline of PbO_2 (see Fig.2), and are hardly reacted with fluorine ions in the aqueous solution, due to lead dioxide more stable than tetrafluoride lead in aqueous solution [23]. From the combined evidences of XRD (see Fig.2) and SEM (see Fig.1), oxide film for all oxidation time contains PbO, which is easily reacted with fluorine ions to form PbF_2, leading to loosenness and porosity of oxide film. This cause that the dioxide layer for further oxidation has a tendency to crack or break from the lead alloys anode, exposing the underneath fresh lead surface to the electrolyte. This explains that anodic peaks in cyclic voltammetry are presented again for oxide films at 2.5h.

After cyclic voltammograms investigations, samples were also investigated by electrochemical impedance (EIS) so as to gain a better electrochemical understanding of the electrolyte-lead alloys anode interface. Spectra of 0, 0.5, 1, 1.5, 2 and 2.5h oxidised surfaces of lead alloys anode were recorded and Nyquist plots for these samples are shown in Fig.5. EIS experiments for the new lead anode in Cr solution show one capacitive loops in high and middle frequency (HF and MF), and an inductive loop at very low frequencies.

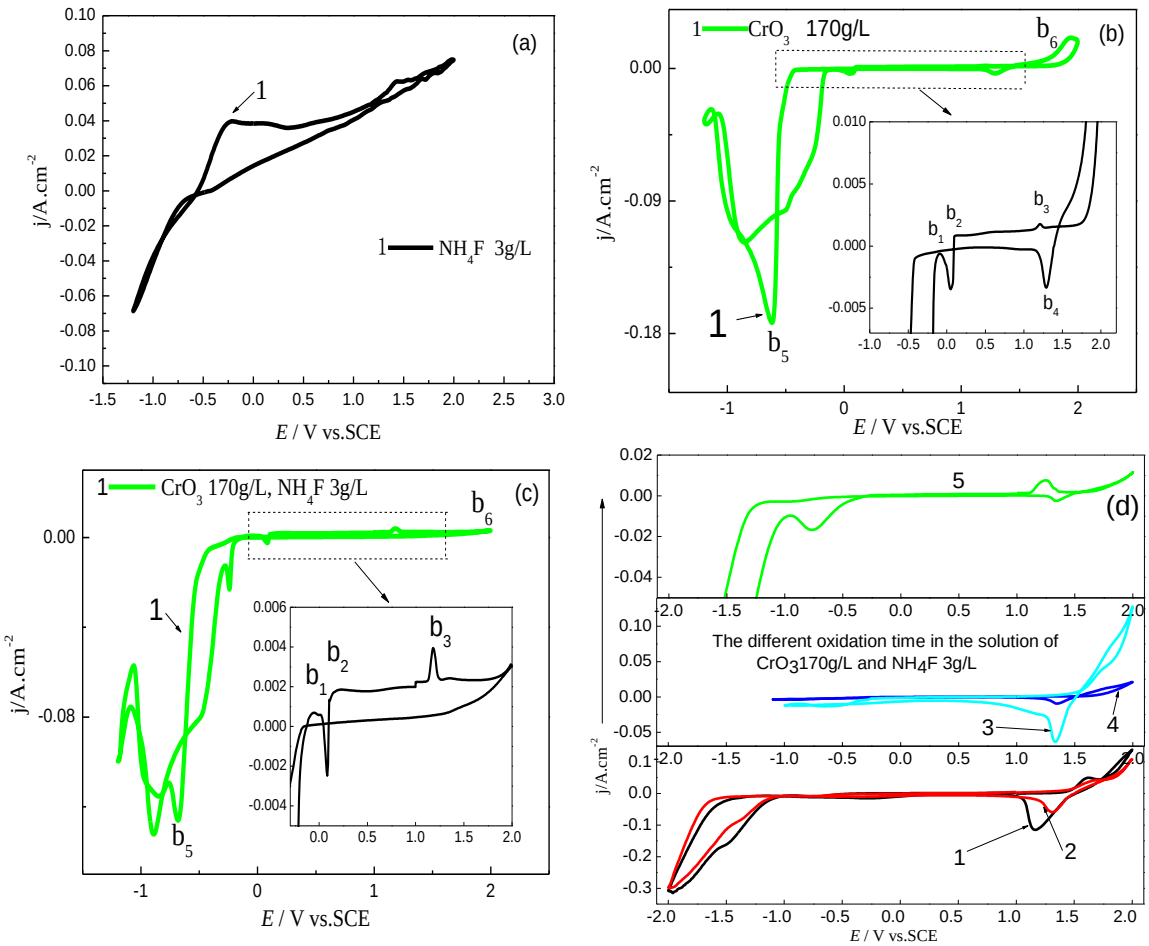

Figure 4. CV curves of (a), (b), (c) the new lead anode lead alloy, and (d) lead anode with oxide film under different oxidation time of 1-0.5h, 2-1.0h, 3-1.5h, 4-2.0h and 5-2.5h

HF and MF capacitive loops are usually attributed to both charge transfer and the double layer associated with the interface between the electrolyte and the lead alloys anode surface. According to G. Baril et al. report [24], these loops are the relaxation of mass transport in the growing solid oxide phase. In Fig. 5(a), a clear trend is observed in the charge transfer resistance R_t (*i.e.*, the diameter of the Nyquist curve along the real axis). The value of R_t is about ~330Ω for the sample in 170g/L CrO_3 solution. In the case of low frequencies loops, the EIS results for the samples in 170g/L CrO_3 solution show a complete circle indicating a large inductance. A. Bonnefont et al. [25] suggests that for this set of parameters one of the limiting processes is apparently the adsorption of chromium-oxide ion cluster on the free sites of the lead alloys anode surface. Note, however, that the mechanism giving rise to ion clusters is rather complex and the rate of another process, the surface reaction between adsorbed chromium-oxide ions cluster and lead alloy hydroxide, decreases also significantly at this modulation frequency. In addition, strong inductive loops are reported due to high concentrations of ions on relatively film-free surface [26]. But the low-frequency (LF) inductive loops disappear and are substituted by a Warburg impedance when the fluorine ions are added into chromium-included solution. This indicates that fluorine ions have a progressive effect on adsorption actions resistance of chromium-oxide ions cluster. Through fluoride activation of the surface by steeping in fluorine-

included solution, which leads to the formation of a thin fluoride passivating layer, the adsorption of chromium-oxide ions cluster on the free sites of the lead alloys anode surface becomes damaged from the solution-surface removing the faradaic inductance. Furthermore, the F^- passivating layer creates a resistance in series with the original surface increasing the charge transfer resistance.

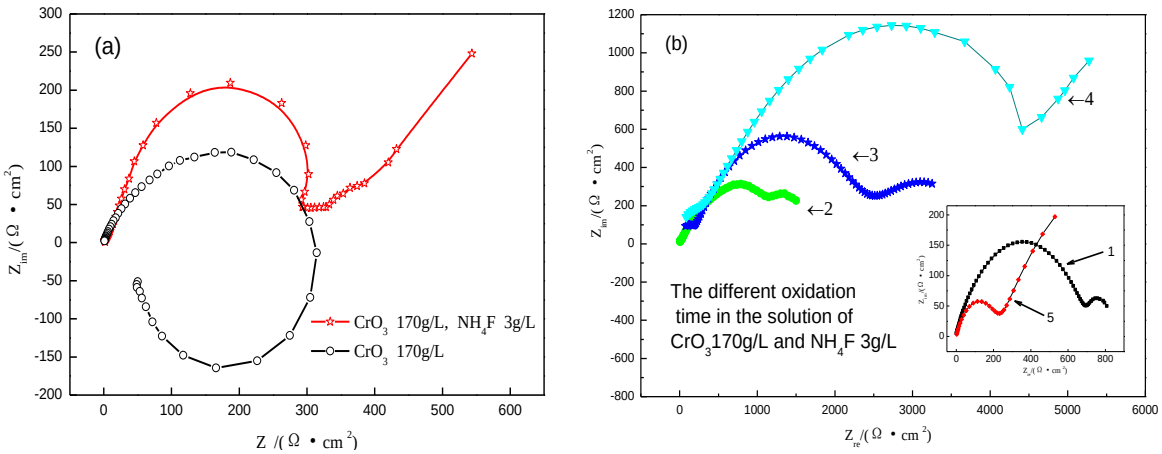

Figure 5. Nyquist curves of (a) the new lead anode lead alloy, (b) lead anode with oxide film under different oxidation time of 1-0.5h, 2-1.0h, 3-1.5h, 4-2.0h and 5-2.5h

EIS results for lead anode with oxide films at 0.5, 1 and 1.5h, respectively, in Cr-F solution show two capacitive loops in the high, middle and low frequency domain. Although the capacitive loops in the MF and LF region of three the curves are small, they are always apparent. For MF and LF capacitive loops, proposals are reported by Song et al. According to Song et al. [27], these loops are attributed to chromium or fluorine ions concentration within the broken areas of surface-oxide film. In Fig. 5(b), a clear trend is also observed in the charge transfer resistance R_t. The value of R_t increase from ~800Ω for the 0.5h oxidised sample to ~3200Ω for the 1.5h oxidised sample. In addition, for lead anode with oxide film at 2 and 2.5h, respectively, the diagram is characterized by one capacitive loop and a Warburg line. For a Warburg line, which is introduced to describe the low frequency part of the impedance diagram, the charge transfer seems to be controlled by a dissolution mechanism [28]. For our results, the Warburg impedance in LF domain indicates oxide films for further oxidation have developed many cracks and fissures, and provide the channels of ions diffusion. This deterioration in the surface of the 2.5h sample may facilitate the lower corrosion resistance, due to the value of R_t lower than that of others at 0.5, 1, 1.5 and 2h.

4. CONCLUSIONS

From the reults above, the following conclusions can be drawn.

(1) After above 0.5h oxidation in Cr-F solution under current density of 20A/dm^2, the oxide film on lead alloys anode electrochemically developed a double-layer oxide structure with outer layer of primarily PbO and PbO_2 atop the inner layer of $PbCrO_4$ and PbF_2, followed by PbO. And $PbCrO_4$

and PbF_2 were observed to play an important role before and after oxide film containing PbO and PbO_2 to crack or break from the lead alloys anode.

(2) In the initial oxidation stage of lead alloys anode for oxidation time below 60s, the PbF_2 wase found to be a very imporant composition resulting in changes to the different distribution of $PbCrO_4$ and PbO on the anode surface.

(3) Cyclic voltammetry and electrochemical impedance spectroscopy (EIS) were used to give a detailed description of the corrosion mechanisms of lead alloys anode in Cr-F solution under electric field. PbO in oxide film was easily eroded by fluorine ions in Cr-F solution under electric field , but a better crystalline of PbO_2 was hardly reacted with fluorine ions in Cr-F solution, due to lead dioxide more stable than tetrafluoride lead in aqueous solution. This led to lead alloys anode degraded rapidly, becuase the outer layer of oxide film containing PbO.

ACKNOWLEDGEMENTS
This work was financially supported by the National Natural Science Foundation of China (51004028) and the Special Fund for Basic Scientific Research of Central Colleges (N100402002).

References

1. D. Devilliers, M.T. Dinh Thi, E. Mahé, Q. Le Xuan, *Electrochim. Acta* 48 (2003) 4301.
2. Y. Li, L.X. Jiang, X.J. Lv, Y.Q. Lai, H.L. Zhang, J. Li, Y.X. Liu, *Hydrometallurgy* 109 (2011) 252.
3. A.M. Lafront,W. Zhang, E. Ghali, G. Houlachi, *Electrochim. Acta* 55 (2010) 6665.
4. D.R.P. Egan, C.T.J. Low, F.C. Walsh, *J. Power Sources* 196 (2011) 5725.
5. W. R. Osório, L. C. Peixoto, A. Garcia, *J. Power Sources* 194 (2009) 1120.
6. I. Ivanov, Y. Stefanov, Z. Noncheva, M. Petrova, Ts. Dobrev, L. Mirkova, R. Vermeersch, J.-P. Demaerel, *Hydrometallurgy* 57(2000)109.
7. F. A. Pérez-González, C. G. Camurri, C. A. Carrasco, R. Colás, *Materials Characterization* 64 (2012) 62.
8. D.G. Li, G.S. Zhou, J. Zhang, M.S. Zheng, *Electrochim. Acta* 52 (2007) 2146.
9. T. Hirasawa, K. Sasaki, M. Taguchi, H. Kaneko, *J. Power Sources* 85 (2000) 44.
10. J. Xu, X.B. Liu, X.G. Li, E. Barbero, C.F. Dong, *J. Power Sources* 155(2006) 420.
11. F. Hine, K. Takayasu, N. Koyanagi, *J. Electrochem. Soc* 133(1986)346.
12. M.J.P. McBurney, D.R. Gabe, *Surf. Tech.* 9(1979)253.
13. C. Rerolle, R.Wiart, *Electrochim. Acta* 41(1996) 1063.
14. I. Ivanov, Y. Stefanov, Z. Noncheva, M. Petrova, Ts. Dobrev, L. Mirkova, R. Vermeersch, J.-P. Demaerel, *Hydrometallurgy* 57(2000)125.
15. W. Zhang, G. Houlachi, *Hydrometallurgy* 104 (2010) 129.
16. Y.Q. Lai, L.X. Jiang, J. Li , S.P. Zhong, X.J. Lü, H.J. Peng, Y.X. Liu, *Hydrometallurgy* 102 (2010) 73.
17. L. Lu, T.C. Liu, X.G. Li, *Surf. Coat. Tech.* 202(2008)1401.
18. M. M. Hoffmann, J. G. Darab, J. L. Fulton, *J. Phys. Chem.* A 105 (2001) 1772.
19. J. Z. Li, X.L. Sun, Y.W. Tian, Y. Zhao, *J. Electrochem. Soc* 160 (2013) (Accepted).
20. P.Thangadurai, S. Ramasamy, R. Kesavamoorthy, *J. Phys.:Condens. Matter* 17(2005)863.
21. E. Bandiello, D. Errandonea, D. Martinez-Garcia, D. Santamaria-Perez, F.J. Manjón, *Physical Review B* 85 (2012) 1.
22. D.G. Li, S.G. Zhou, *Acta Chimica Sinica* 66 (2008) 617.

23. J. Bornstein, L. Skarlos, *J. Am. Chem. Soc.* 90(1968)5044.
24. G. Baril, C. Blanc, M. Keddam, N. Pébère, *J. Electrochem. Soc.* 150 (2003) B488.
25. A. Bonnefont, R. Morschl, P. Bauer, K. Krischer, *Electrochim. Acta* 55 (2009) 410.
26. G. Baril, G. Galicia, C. Deslouis, N. Pebere, B. Tribollet, V. Vivier, *J. Electrochem. Soc.* 154(2007)C108.
27. G. Song, A. Atrens, X. Wu, B. Zhang, *Corros. Sci.* 40(1998)1769.
28. S.Chauffaille, O. Devos, J.Jumel, M.E.R. Shanahan, *Int. J. Adhes. Adhes.* 30(2010)602.

© 2013 by ESG (www.electrochemsci.org)